

Original Paper

CO₂ and HCO₃⁻ Permeability of the Rat Liver Mitochondrial Membrane

Mariela Arias-Hidalgo^a Jan Hegermann^b Georgios Tsiavaliaris^c Fabrizio Carta^d
Claudiu T. Supuran^d Gerolf Gros^a Volker Endeward^a

^aAbt. Molekular- und Zellphysiologie, AG Vegetative Physiologie 4220, Medizinische Hochschule Hannover, Hannover, ^bAbt. Funktionelle und Angewandte Anatomie, Elektronenmikroskopie 8840, Medizinische Hochschule Hannover, Hannover, ^cAbt. Biophysikalische Chemie 4350, Medizinische Hochschule Hannover, Hannover, Germany; ^dNEUROFARBA Dipart., Pharmaceutical and Nutraceutical Chemistry, University of Florence, Sesto Fiorentino, Italy

Key Words

CO₂ permeability • Membrane cholesterol • Gas channels • Mitochondria • Rat liver • ¹⁸O exchange technique

Abstract

Background/Aims: Across the mitochondrial membrane an exceptionally intense exchange of O₂ and CO₂ occurs. We have asked, 1) whether the CO₂ permeability, P_{M,CO₂}, of this membrane is also exceptionally high, and 2) whether the mitochondrial membrane is sufficiently permeable to HCO₃⁻ to make passage of this ion an alternative pathway for exit of metabolically produced CO₂. **Methods:** The two permeabilities were measured using the previously published mass spectrometric ¹⁸O exchange technique to study suspensions of mitochondria freshly isolated from rat livers. The mitochondria were functionally and morphologically in excellent condition. **Results:** The intramitochondrial CA activity was exclusively localized in the matrix. P_{M,CO₂} of the inner mitochondrial membrane was 0.33 (SD ± 0.03) cm/s, which is the highest value reported for any biological membrane, even two times higher than P_{M,CO₂} of the red cell membrane. P_{M,HCO₃} was 2·10⁻⁶ (SD ± 2·10⁻⁶) cm/s and thus extremely low, almost 3 orders of magnitude lower than P_{M,HCO₃} of the red cell membrane. **Conclusion:** The inner mitochondrial membrane is almost impermeable to HCO₃⁻ but extremely permeable to CO₂. Since gas channels are absent, this membrane constitutes a unique example of a membrane of very high gas permeability due to its extremely low content of cholesterol.

© 2016 The Author(s)
Published by S. Karger AG, Basel

Introduction

Mitochondria, the organelles responsible for cellular respiration, convert O₂, ADP and energy substrates into ATP, CO₂ and water. Their O₂ consumption together with their - about identical - CO₂ production requires that both gases meet no major diffusion resistance

Dr. Gerolf Gros

Abt. Molekular- und Zellphysiologie, AG Vegetative Physiologie – 4220 –Medizinische Hochschule Hannover, 30625 Hannover, (Germany)
Fax +49-511-532 2938, E-Mail Gros.Gerolf@MH-Hannover.de

KARGER

when passing through the mitochondrial membrane from/into the mitochondrial matrix. While the O₂ permeability of the mitochondrial membrane has not been accessible to direct determination, Elder and Lehninger [1] and Balboni and Lehninger [2] have presented qualitative evidence indicating that the inner mitochondrial membrane is permeable to CO₂ but not to HCO₃⁻. In view of the extremely high rate of CO₂ production per mitochondrial volume, one must postulate then that the mitochondrial membrane possesses an unusually high permeability for CO₂. We ask here whether and by which mechanism the mitochondrial membrane does indeed achieve a high permeability to CO₂. This question arises, because several biological membranes have been reported to possess low CO₂ permeabilities (0.017 cm/s for the cell lines MDCK and tsA201, or even 0.0015 cm/s for the apical membrane of colonic epithelium [3, 4]). Others, such as the red blood cell membrane, on the other hand possess a much higher CO₂ permeability of 0.15 cm/s [5, 6].

For methodological reasons, it has so far not been possible to determine the permeability of the mitochondrial membrane for CO₂ quantitatively. Only more recently, the mass spectrometric ¹⁸O exchange technique developed in our lab [4] has made it feasible to tackle this problem. This method is suitable to determine P_{M,CO₂} and P_{M,HCO₃⁻} not only of cells but also of vesicles and organelles [3, 7]. Thus, we determine here the CO₂ permeability along with the bicarbonate permeability of the mitochondrial membrane.

We wanted to answer two questions: 1) Does the mitochondrial membrane indeed possess a very high CO₂ permeability as expected from its exceptionally high rate of CO₂ exchange? 2) If the CO₂ permeability does turn out to be very high, what is the mechanistic basis for this property in view of other less permeable biological membranes? 3) Does the bicarbonate permeability of the mitochondrial membrane allow a significant permeation of HCO₃⁻, as an alternative pathway to CO₂? This latter question is still controversial, as Vincent and Silverman [8] have reported a high HCO₃⁻ permeability, similar to that of the human red blood cell membrane, while Dodgson et al. [9] find a value at least two orders of magnitude lower than found in red cells.

Materials and Methods

Solutions

Homogenization medium (HM buffer). 0.32 M Sucrose, 1 mM EDTA and 10 mM Tris-HCl and pH adjusted to 7.4.

O₂ and CO₂ Buffers. The "O₂ buffer" (for measurement of mitochondrial O₂ consumption) consists of 125 mM KCl, 20 mM MOPS, 5 mM KH₂PO₄ and 1 mM MgCl₂. The "CO₂ buffer" (for the measurement of ¹⁸O exchange) consists of the same components as the O₂ buffer, but has 25 mM KCl less [10]. Both buffers were filtered through a Millipore filter with pore size 0.2 μm.

Lysate Buffer. 60 mM NaCl, 20 mM Hepes, 23.7 mM HSO₄ and pH adjusted to 7.4.

Isolation of Mitochondria

All experiments were performed using male Lewis rats between 250 and 300 g of body weight with permission of the local authorities for animal experimentation. Animals were anesthetized with carbon dioxide and killed by cervical dislocation. The liver was removed within 5 minutes, washed with ice cold homogenization medium, cut into pieces and homogenized with a Potter-Elvehjem homogenizer. Homogenization and centrifugation steps were performed as described by Fernandez-Vizarra et al. [11, 12].

An initial centrifugation step was performed at 1000 g for 5 min at 4°C and supernatant was taken and aliquots transferred into several 1.5 ml Eppendorf tubes. These samples were then centrifuged at 15,000 g for 2 min at 4°C, supernatant was discarded and the pellets of 2 tubes were combined and resuspended in HM buffer. This process was repeated until there was only one tube containing the entire sample. This tube was centrifuged once more, the supernatant was discarded and the pellet was resuspended in O₂ buffer to be used for further experiments.

Characterization of the mitochondrial samples

Protein content. The final mitochondrial pellet was resuspended in O₂ buffer to a volume of 1000 µl. 10 µl of this suspension were taken for determination of protein content using the Total Protein Kit, Micro Lowry, Peterson's Modification, from Sigma (Sigma-Aldrich, Taufkirchen, Germany). Two determinations of protein content were performed for each sample.

Parameters. We used the protein concentrations of the mitochondrial suspensions to derive mitochondrial matrix volume and inner membrane surface area from the data published by Schwerzmann et al. [13], using their numbers of 1.6 µl/mg protein for matrix volume and 521 cm²/mg protein for inner membrane surface area. The protein concentration of the suspensions was also used to determine the number of mitochondria per volume, using the figure 8.7·10⁹ mitochondria per mg of mitochondrial protein [13].

Electron microscopy. The final mitochondrial pellet was resuspended in a 10-fold volume of fixation buffer (150 mM HEPES, pH 7.35, containing 1.5 % formaldehyde and 1.5 % glutaraldehyde) at RT. Fixation was 30 min at RT and overnight at 4°C. Mitochondria were postfixed in 1% osmium tetroxide 2 h at RT and 4% uranyl acetate at 4°C overnight. After dehydration in acetone, samples were embedded in EPON. 50 nm thick sections were poststained with 4% uranyl acetate and lead citrate [14] and observed in a Morgagni TEM (FEI), operated in the bright field mode. Images were recorded at 80 kV using a 2K side mounted Veleta CCD camera, binned to 1K.

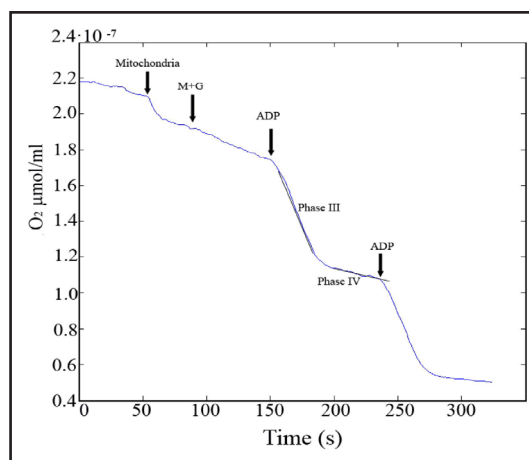
Dynamic Light scattering (DLS). DLS studies were performed using a Viscotek 802 instrument (Viscotek Corporation) equipped with a single mode fiber optics and a 50 mW diode laser (λ = 832 nm) at 20°C. The mitochondrial preparation was diluted 1000-fold in O₂ buffer containing 0.1 %w/v BSA. Prior to dilution the O₂ buffer was filtered through a syringe filter (Minisart®) with a pore size of 0.2 µm (Sartorius, Germany). Polystyrene beads of 1 µm diameter (Molecular probes) and a concentration of 1 × 10⁷ beads per ml were used as a control. The purity of the mitochondrial suspension was estimated from the area of the mitochondrial peak fraction relative to the total area of all peak fractions including that of the contaminants.

Mass spectrometric assays

A chamber with a volume of 2.2 ml was used that was attached to the high vacuum of the mass spectrometer via the previously published inlet system [4]. This chamber had a water-jacket that kept the solutions at 37°C, and contained a stirrer that mixed the content continuously. The pH was adjusted to 7.4 and monitored during the whole procedure with a pH electrode. 50 µl of mitochondrial suspension was used in each experiment.

Oxygen consumption. O₂ consumption of mitochondrial suspensions was measured by monitoring over time the concentration of physically dissolved O₂ in the fluid of the mitochondrial suspension in the mass spectrometer's chamber. The O₂ signal produced by the mass spectrometer was proportional to the O₂ concentration in the sample. Initially, the sample was equilibrated with air. After the chamber was closed, a decline of O₂ concentration in the sample occurred due to mitochondrial respiration and was recorded via the mass spectrometer. The slopes of the recordings represent the O₂ consumption \dot{V}_{O_2} . Each measurement consisted of the following phases, as seen in Fig. 1: (1) \dot{V}_{O_2} of the suitably diluted native mitochondrial

Fig. 1. Original mass spectrometric recording of an oxygen consumption measurement of a mitochondrial suspension. Substrates 5mM glutamate and 1mM malate (second arrow) and 0.3 mM ADP (third and fourth arrow) were added. RCR was calculated using the ratio between oxygen consumption values of the state III (after addition of ADP) and state IV (after ADP has been consumed).



suspension, (2) \dot{V}_{O_2} after addition of glutamate and malate to give final concentrations of 5 and 1 mM, respectively, (3) \dot{V}_{O_2} after addition of ADP at a final concentration of 0.3 mM (giving state III respiration), (4) \dot{V}_{O_2} after the added ADP has been consumed (giving state IV respiration). Specific \dot{V}_{O_2} values and the respiratory control ratio (RCR = slope of state III / slope of state IV) allowed us to assess the functional integrity of the mitochondria [10].

Estimation of CO₂ permeability. The mass spectrometric chamber was filled with isotonic "CO₂ buffer" that contained 25 mM ¹⁸O-labelled HCO₃⁻ as described before [4]. The pH was adjusted to 7.40 at 37°C. The mass spectrometer followed the concentration of C¹⁸O¹⁶O in the chamber fluid. Due to the exchanges of ¹⁸O with water, the C¹⁸O¹⁶O concentration declined over time. After addition of the mitochondrial sample into the chamber, this decline was accelerated, yielding a first fast phase followed by a second slower phase, as is seen in Fig. 4. The acceleration was due to the exchange of ¹⁸O between the pools of CO₂ and water inside the mitochondria, which was sped up by intramitochondrial carbonic anhydrase (CA). After the second phase of C¹⁸O¹⁶O decline had been recorded for a sufficiently long time, a high concentration of CA was added to the chamber to establish final isotopic equilibrium (see Fig. 4). The two phases after addition of mitochondria seen in Fig. 4 were used to derive the CO₂ permeability (P_{M,CO₂}) of the mitochondrial membrane in the manner described previously [4].

Inhibitors used in several experiments were: extracellular carbonic anhydrase inhibitor 2,4,6-trimethyl-1-(4-sulfamoyl-phenyl)-pyridinium perchlorate salt (FC5-208A; [15]) in a final concentration of 2.5·10⁻⁵ M, and the inhibitor of the gas channels aquaporin-1 and RhAG 4,4'-Diisothiocyanato-2,2'-stilbenedisulfonate (DIDS) in a final concentration of 1.0x10⁻⁴ M [16, 6]. Mitochondrial samples were preincubated with inhibitor(s) for 5 min.

Determination of intramitochondrial carbonic anhydrase activity. Mitochondria were kept frozen overnight and thawed the next day. 1 µl of Triton 10% was added to each 100 µl of mitochondrial suspension. 22 µl of the same Triton solution were also added into the measuring chamber of the mass spectrometer containing "lysate buffer" with 25 mM labelled bicarbonate. The experiment was then terminated by the addition of excess CA to establish final isotopic equilibrium. This record was analyzed to obtain the carbonic anhydrase activity and then related to the mitochondrial volume estimated for each sample to obtain the activity inside the mitochondrion. CA activity A was defined as acceleration factor (A+1) of the uncatalysed hydration velocity minus 1. In other words, the total rate of CO₂ hydration v_{CO₂} is given by k_{CO₂}·(A+1)·[CO₂], where k_{CO₂} is the uncatalysed rate constant of CO₂ hydration, and [CO₂] is the concentration of dissolved CO₂.

Statistical Analysis

Data are presented as means and ± SD. For comparisons between more than 2 groups with one independent variable, we used one way ANOVA. Dunnett's post-test was used to allow comparisons with the control group.

Results

Characterization of the mitochondrial preparations

We worked with mitochondrial suspensions containing 32 (SD ± 4; n = 8) mg protein/ml. The oxygen consumption (state III) was 97 (SD ± 38; n = 28) nmol O₂/min/mg protein and the RCR was around 10 (SD ± 5; n = 8). State three respiration rates and RCR values were in the range of literature values for liver mitochondria [10, 13, 17, 18]. In transmission electron microscopy, the mitochondria appeared morphologically intact and little other material was seen (Fig. 2). The average shortest diameter of the mitochondrial profiles obtained by electron microscopy was 0.73 (SD ± 0.11, n=18) µm (the average longest diameter was 0.89 (SD ± 0.13) µm). In addition, we determined the size of the mitochondria by DLS. Fig. 3B shows a measurement of a preparation yielding an average radius of 0.44 (SD ± 0.12) µm (Fig. 3B). Averaging the radii from several DLS measurements using different dilutions of the mitochondrial suspension and various scanning rates of acquisition gave a final diameter of 0.98 (SD ± 0.18, n = 12) µm. The short diameter of 0.73 µm from electron microscopy is in excellent agreement with the value given by Schwerzmann et al. [13], and all

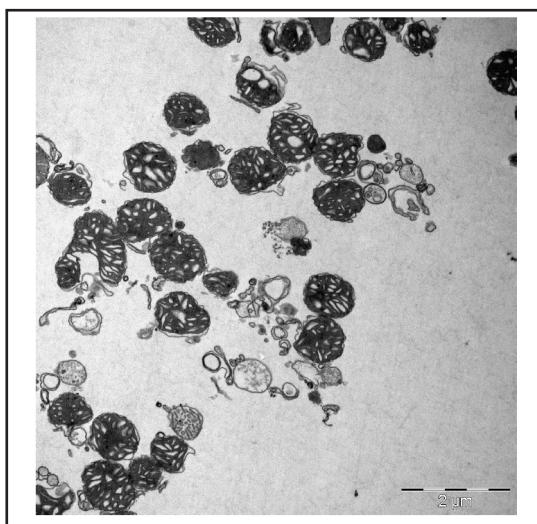


Fig. 2. Electron microscopic image of isolated mitochondria. Their shape and structure are well preserved, and only moderate contamination with other membranes or other cellular components is found. Complete bar = 2 μm.

diameters mentioned are in the range given in the literature [19]. In addition to the overall radius, the DLS measurement allows us by quantification of the areas of the DLS peaks to give an estimate of the purity of the sample. This value was approximately 70%, a figure compatible with the degree of purity seen in the electron micrograph of Fig. 2. This is considered a very satisfactory degree of purity.

Determinations of mitochondrial CO₂ and HCO₃⁻ permeability

Among the measurements of ¹⁸O-exchange in mitochondrial suspensions (Fig. 4), we performed 32 experiments with control conditions, and 12 with each of the inhibitors, FC5-208A and DIDS, respectively. The CO₂ permeability values obtained from the fitting procedure [4] were either between

0.3 and 0.4 cm/s, or they were > 400 cm/s and did not reach convergence. This shows that a) the permeability of the mitochondrial membrane is > 0.3 cm/s, b) it may be even higher than 0.4 cm/s, but this cannot be demonstrated because the method becomes insensitive to P_{M,CO2} above ~ 0.4 cm/s. In the case of control measurements of mitochondria in the absence of inhibitors, 8 out of 32 measurements did not converge and P_{M,CO2} in these 8 measurements thus appeared to be > 0.4 cm/s. In the presence of the extracellular CA inhibitor FC5-208A 2 out of 12 measurements did not converge, and in the case of experiments in the presence of DIDS 7 out of 12 measurements did not converge. The results shown in Fig. 5 are based on the P_{M,CO2} values obtained up to a value of about 0.4 cm/s. So, in most cases, the calculated P_{M,CO2} values range between 0.3 and 0.4 cm/s. Thus, at least in the control experiments and those in the presence of FC5-208A, the means given in Fig. 5 should be fairly reliable and the

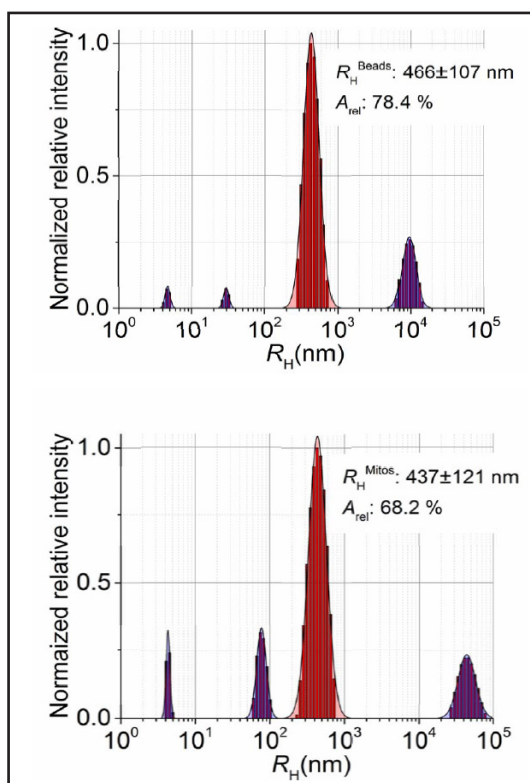


Fig. 3. DLS experiments of radii distribution and relative abundance of particles. (A) Size distribution histogram of polystyrene beads reveal a mean average radius of $0.47 \pm 0.11 \mu\text{m}$, which agrees well with the manufacturer's specification when taking the uncertainty of the DLS derived intensity size distribution of approximately 10 to 15% into account. (B) Representative size distribution histogram of a mitochondrial preparation. The mean average radius of the mitochondria is $0.44 \pm 0.12 \mu\text{m}$ (main peak distribution). Low and high molecular weight contaminations of the mitochondrial preparation with proteins and other cellular components are shown as distributions of the minor peaks. The error corresponds to the half-width of the peak size. The relative purity of the mitochondrial preparation is found to be approximately 70%.

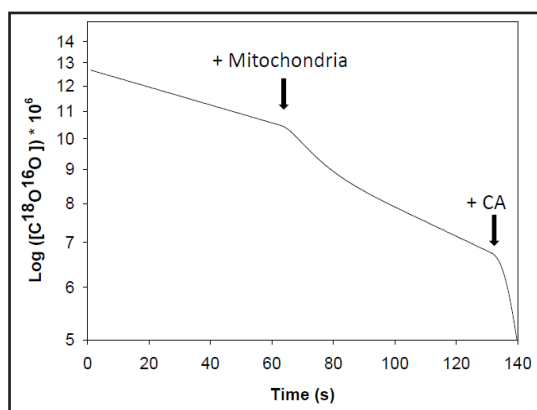


Fig. 4. Original mass spectrometric recording of an experiment with rat liver mitochondria. Mass 46 (C¹⁸O¹⁶O) is plotted logarithmically versus time. 1st arrow indicates addition of mitochondrial suspension to reaction chamber, 2nd arrow indicates addition of an excess of carbonic anhydrase to establish final isotopic equilibrium.

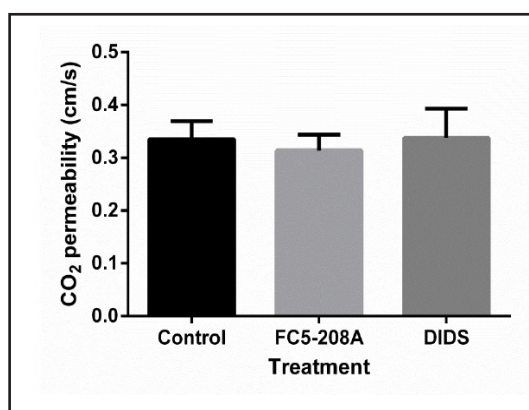


Fig. 5. CO₂ permeability of mitochondria in suspension and the effect of extracellular CA inhibitor FC5-208A (2.5·10⁻⁵ M) and the CO₂ channel inhibitor DIDS (1.0·10⁻⁴ M). ANOVA p = 0.29. From left to right n = 24, n = 10, n = 5. Bars represent SD.

true values should not be significantly higher than shown.

From control experiments, we calculated a mean bicarbonate permeability of 2·10⁻⁶ cm/s (SD ± 2·10⁻⁶ cm/s, n = 39). This is a very low value compared to red cells [6] but it is still significantly different from 0 (p < 0.0001). Mean intra-matrix CA activity was found to be 675 (SD ± 151, n = 8). This activity is high, yet still a little less than 5% of the exceptionally high human intraerythrocytic CA activity.

The mitochondrial CO₂ permeability we obtain under control conditions is 0.33 cm/s (SD ± 0.03; n = 24; Fig. 5), which is twice as high as the value of 0.15 cm/s reported for the human red cell membrane [5, 6]. Because extracellular CA activity could interfere with the P_{M,CO₂} calculations, we performed experiments in the presence of FC5-208A, a membrane-impermeable and thus extracellular and extramitochondrial CA inhibitor. Organelles pre-incubated with FC5-208A exhibit the same permeability of 0.32 cm/s (SD ± 0.03; n = 10), indicating that no extramitochondrial CA is present in our mitochondrial suspensions. Finally, we performed experiments with DIDS, a CO₂ channel inhibitor (of aquaporin 1 and RhAG [5, 6, 16]), and obtained a P_{M,CO₂} of 0.34 cm/s (SD ± 0.06; n = 5), again identical to control P_{M,CO₂}.

Discussion

Stereological Mitochondrial Parameters

The calculation of P_{M,CO₂} from the two phases of C¹⁸O¹⁶O decline seen in Fig. 4 requires knowledge of the mitochondrial matrix volume and the surface of the inner mitochondrial membrane [4]. These values have been determined for rat liver mitochondria by Schwerzmann et al. [13], who report a matrix volume of 1.6 μl/mg mitochondrial protein and a surface area of the inner membrane of 521 cm²/mg protein. Matrix volume rather than total mitochondrial volume and inner membrane rather than outer mitochondrial membrane were chosen, because a) all mitochondrial CA is present in the matrix (see below), and b) the outer mitochondrial membrane has large pores and thus is less likely to offer a significant resistance towards permeation of CO₂ as well as HCO₃⁻ in comparison to the inner mitochondrial membrane. For the mitochondrial matrix volume, various estimates have been obtained. Besides the value employed here, 1.6 μl/mg protein as reported by Schwerzmann et al. [13], Halestrap and Quinlan [20] obtained values of 0.46 and 1.68 μl/mg

(where they preferred the estimate of 0.46 $\mu\text{l}/\text{mg}$). Cohen et al. [21] reported matrix volumes between 0.85 and 1.4 $\mu\text{l}/\text{mg}$, and Vincent and Silverman [8] found a value of 1.4 $\mu\text{l}/\text{mg}$. We tested the effect of assumed matrix volumes of 1 $\mu\text{l}/\text{mg}$ and 0.46 $\mu\text{l}/\text{mg}$ on the calculated CO₂ permeabilities, and found for both these values average P_{M,CO_2} values remaining between 0.2 and 0.4 cm/s, i.e. very similar to the P_{M,CO_2} value calculated with a matrix volume of 1.6 $\mu\text{l}/\text{mg}$. Thus, the P_{M,CO_2} values of Fig. 5 do not depend very much on the value chosen from this range of mitochondrial matrix volumes. This is due to the fact that, at the given experimental CA activity of the mitochondrial lysate, the calculated intra-matrix CA activity increases as mitochondrial volume decreases, and these two changes largely compensate each others' opposite effects on P_{M,CO_2} .

Imperfect Purity of Mitochondrial Preparation

As discussed above, the present mitochondrial preparation is not entirely pure, the contaminations amounting to 30% according to DLS measurements (Fig. 3). On the other hand, we use here the mitochondrial parameters derived from another study, that of Schwerzmann et al. [13], which raises the question to which extent their parameters are applicable to our preparations. A first consideration concerns the present preparation technique. This technique is almost identical to the one used by Schwerzmann et al. [13], with one major exception: we did not include the final step used by Schwerzmann et al. [13], Percoll gradient centrifugation intended to reduce microsomal contamination. We tested the effect of this step and found no improvement of the purity of the preparation, but an impairment of the functional properties of the mitochondria after Percoll. Therefore, this step was omitted. This suggests that the purity of the present preparation may be similar to that of Schwerzmann et al. [13]. A second consideration concerns the hypothesis that the data of Schwerzmann et al. [13] refer to a 100% pure preparation, while 30% of the protein of our preparation is not due to mitochondria. Which error in our estimate of P_{M,CO_2} would this situation cause? 30% contaminating proteins would reduce the mitochondrial volume and surface as calculated from Schwerzmann's data [13] by 30%, and at the same time increase calculated intra-matrix CA activity by 30%. As mentioned above, the reduction in volume and the increase in activity largely compensate each other, such that the average P_{M,CO_2} of a representative group of experiments is calculated to fall from 0.32 cm/s to 0.29 cm/s, an error negligible in view of the limitations of the present method. In conclusion, even if there is a major difference between the purities of the preparations of Schwerzmann et al. [13] and of this paper, this has no relevant effect on the value of mitochondrial P_{M,CO_2} . The same holds for P_{M,HCO_3^-} .

Mitochondrial Carbonic Anhydrase Activity

For rat liver mitochondria at 37°C we report here an intra-matrix CA activity of 675, indicating that the intra-matrix rate of CO₂ hydration is accelerated over its uncatalysed value by a factor 675+1 = 676. For guinea pig liver mitochondria at 25°C, Dodgson et al. [9] have reported a standard k_{cat} of 0.13 ml/s/mg protein. Using the above matrix volume of 1.6 $\mu\text{l}/\text{mg}$, this gives an activity of 2030 in the matrix of these mitochondria. The difference between this value and the present one can be due to the difference in species and/or to the difference in temperatures. For rat liver mitochondria at 25°C, Vincent and Silverman [8] report a mitochondrial CA activity of 700, very similar to our value at 37°C. However, they conclude from digitonin subfractionation experiments that about one half of this CA activity is located in the space between inner and outer mitochondrial membrane, and only the other half in the matrix. We cannot confirm this latter conclusion, as the membrane-impermeable inhibitor FC5-208A (mol.wt. 376.81) should be able to enter the space between the two membranes through the porins but should not have access to the intra-matrix space. As apparent from Fig. 5, FC5-208A has no effect on calculated CO₂ permeability, which means that the mass spectrometric signal is not detectably altered by the presence of FC5-208A. If there were significant extra-matrix CA in these mitochondria, we would expect a marked change of the mass spectrometric signal upon addition of the inhibitor. Thus, the present

results yield CA activities that are in a range similar to previously reported values, but show that CA is localized entirely in the mitochondrial matrix space. The latter conclusion is in agreement with the observations of Balboni and Lehninger [2], who observed that rat liver mitoplasts, which are devoid of the outer mitochondrial membrane and the intermembrane space, exhibit a similar rapid uptake of CO₂ into the matrix as intact liver mitochondria.

The localization of CA within the mitochondrion is relevant for the present study, because the ¹⁸O exchange technique observes the exchange of CO₂ and HCO₃⁻ between the compartment containing the CA and the surrounding space devoid of CA [7]. If the space containing the CA is the matrix, and both the space between the two mitochondrial membranes and the extramitochondrial space are free of CA, then the permeabilities measured here for CO₂ as well as HCO₃⁻ should refer to the sum of the diffusion resistances of the inner and the outer mitochondrial membrane. In view of the fact that the outer membrane has large pores and is known to be quite permeable, it is likely that our permeability results essentially reflect the properties of the inner mitochondrial membrane.

Low Mitochondrial Bicarbonate Permeability

Williams [22] has early on postulated that it is HCO₃⁻ rather than that CO₂ leaves the mitochondrial matrix. Elder & Lehninger [1] and Balboni and Lehninger [2] have presented several lines of evidence indicating that it is more likely that CO₂ is the permeating species. In view of this discussion it is of interest to know what the permeability of the (inner) mitochondrial membrane for HCO₃⁻ is. This question has been studied by Dodgson et al. [9], who used the same ¹⁸O-exchange technique that we apply here. Their approach differs from the present one by the theoretical treatment. They consider the membrane permeability for CO₂ to be infinite and derive the two parameters intramitochondrial CA activity and membrane bicarbonate permeability from mass spectrometric recordings such as the one shown in Fig. 4 (see method in [23]). In our treatment the intramitochondrial CA activity is determined independently, and the two parameters membrane P_{M,CO₂} and P_{M,HCO₃⁻} are derived from the mass spectrometric recordings [4]. Therefore, the results for P_{M,HCO₃⁻} obtained by Dodgson et al. [9] and in the present paper are not strictly comparable, even if the experimental mass spectrometer recordings were identical. However, since we find here an exceptionally high CO₂ permeability of the mitochondrial membrane, it can be expected that assuming it to be infinite does not affect the calculated value of P_{M,HCO₃⁻} very much. Thus, it is not surprising that our value for P_{M,HCO₃⁻}, 2·10⁻⁶ cm/s, is well within the range of values between 10⁻⁶ and 10⁻⁵ cm/s reported by Dodgson et al. [9]. These values are almost three orders of magnitude lower than the P_{M,HCO₃⁻} of about 10⁻³ cm/s in human red cells, which possess the chloride-bicarbonate exchanger AE1 in their membrane [6, 24, 25]. The present mitochondrial P_{M,HCO₃⁻} of 2·10⁻⁶ cm/s is about as low as the P_{M,HCO₃⁻} of hagfish red cells, which lack the AE1 and have been reported to exhibit a P_{M,HCO₃⁻} of << 10⁻⁵ cm/s [26]. Both bicarbonate permeabilities can be considered to be close to zero. This would be clearly lower than the mitochondrial P_{M,HCO₃⁻} of 9·10⁻⁵ cm/s reported by Vincent and Silverman [8], but would agree with the reports of Chappell and Crofts [27] and Elder and Lehninger [1], who concluded that bicarbonate is virtually impermeable in the inner mitochondrial membrane. In summary, we confirm here the concept of Elder and Lehninger [1] and Balboni and Lehninger [2] that bicarbonate does not play a significant role in mediating the transfer of CO₂ - HCO₃⁻ across the mitochondrial membrane.

High Mitochondrial CO₂ Permeability, Significance and Mechanism

Physiological Significance. If CO₂ is the only form in which all species of the CO₂/HCO₃⁻/H₂CO₃/CO₃²⁻ system can pass the inner mitochondrial membrane, then all CO₂ produced from O₂ inside the mitochondrion has to permeate this membrane in the form of CO₂. If we take oxygen consumptions as an approximation of CO₂ production rates, we can use the state III mitochondrial oxygen consumption measured in this study, $\dot{V}_{O_2} = 97 \text{ nmol O}_2/\text{min/mg}$ protein (see Results). We convert this to \dot{V}_{O_2} per volume using the matrix volume of 1.6 μl/mg, and obtain a \dot{V}_{O_2} per matrix volume of ~ 1000 nmol/s/ml. One can now compare this

figure with the O₂ consumption of a cell line in culture, MDCK, which exhibits a low oxygen consumption of 1.25 fmol/min/cell [28]. Converting this number to \dot{V}_{O_2} per cell volume, we obtain about 12 nmol/s/ml. This is a 100x lower specific \dot{V}_{O_2} than that of mitochondria.

Mitochondria seem to be well adapted to the high \dot{V}_{CO_2} by their high P_{M,CO_2} of 0.3 cm/s, whereas MDCK cells are obviously able to sufficiently release their CO₂, produced at a 100x lower rate, in spite of their much lower P_{M,CO_2} of 0.017 cm/s [3]. However, the size and surface area of a mitochondrion and a MDCK cell are greatly different. In order to obtain a rough estimate of the efficiencies in releasing CO₂ achieved by mitochondria vs. MDCK cells, we can calculate the ratio of whole organelle/cell CO₂ membrane conductance, C_M , over whole cell/organelle CO₂ production, \dot{V}_{CO_2} . Membrane conductances are given by $P_{M,CO_2} \cdot A$, A representing the total membrane area of the single cell or organelle. For mitochondria one obtains $C_M = 0.3 \text{ cm/s} \cdot 6.0 \cdot 10^{-8} \text{ cm}^2 = 1.8 \cdot 10^{-8} \text{ cm}^3/\text{s}$ (A taken from [13]), for MDCK cells $C_M = 0.017 \text{ cm/s} \cdot 7 \cdot 10^{-6} \text{ cm}^2 = 12 \cdot 10^{-8} \text{ cm}^3/\text{s}$ (A calculated from a cell diameter of 15 μm assuming a spherical shape of the MDCK cell). \dot{V}_{CO_2} per mitochondrion with a matrix volume of $1.84 \cdot 10^{-13} \text{ cm}^3$ [13] is obtained from the above \dot{V}_{CO_2} per volume to be $1.84 \cdot 10^{-10} \text{ nmol/s}$. \dot{V}_{CO_2} of a MDCK cell is obtained analogously to be $12 \text{ nmol/s/cm}^3 \cdot 1.77 \cdot 10^{-9} \text{ cm}^3 = 2.1 \cdot 10^{-8} \text{ nmol/s}$ (the cell volume being calculated from the diameter of 15 μm). For the ratio of C_M over \dot{V}_{CO_2} we obtain then for mitochondria: $C_M/\dot{V}_{CO_2} = 1.8 \cdot 10^{-8} \text{ cm}^3/\text{s} / 1.84 \cdot 10^{-10} \text{ nmol/s} = 98 \text{ cm}^3/\text{nmol}$, and for MDCK cells: $C_M/\dot{V}_{CO_2} = 12 \cdot 10^{-8} \text{ cm}^3/\text{s} / 2.1 \cdot 10^{-8} \text{ nmol/s} = 5.7 \text{ cm}^3/\text{nmol}$.

Thus, mitochondria possess an almost 20 times greater membrane CO₂ conductance per rate of CO₂ production than MDCK cells. We conclude that mitochondria possess an especially perfect optimization of CO₂ release across their membranes when compared to MDCK cells. This advantage would disappear, if the mitochondrial membrane had a similarly low CO₂ permeability as MDCK cells have.

Mechanism of High CO₂ Permeability of Mitochondria. Several authors have shown that a major parameter determining the permeability of phospholipid and cell membranes is the cholesterol content of the membrane [3, 29-31]. Itel et al. [3], Kai and Kaldenhoff [30] and Tsiavaliaris et al. [31] have shown that the CO₂ permeability of liposomes and artificial phospholipid membranes – like that of cell membranes – is in addition governed by the presence or absence of membrane gas channels. The content of cholesterol can reduce P_{M,CO_2} from > 0.16 cm/s in the absence of cholesterol to ~ 0.002 cm/s in the presence of 70% mol% cholesterol per total lipids, i.e. by at least two orders of magnitude [3, 29]. This finding implies that cell membranes with a normal cholesterol content of 30-40% can have a rather low CO₂ permeability, such as for example MDCK cells with a P_{M,CO_2} of 0.017 cm/s [3]. In tissues with a high metabolic rate, such as the heart, such a permeability would be limiting for cellular CO₂ release [7]. Thus, it is important that cell membranes in such tissues acquire a substantially higher membrane P_{M,CO_2} . Itel et al. [3] have shown in artificial phospholipid membranes that an effective means to achieve this is to incorporate protein gas channels into the membrane. Incorporating the gas channel aquaporin 1, they were able to increase P_{M,CO_2} in a membrane containing 50 mol% cholesterol up to 10-fold. Thus, in tissues of high metabolic rate P_{M,CO_2} can become high in spite of a high cholesterol content of the membrane, which may be needed for other reasons such as establishing the desired mechanical properties of the membrane [32] or because of cholesterol's general barrier function [33].

The mitochondrial membrane seems to constitute an example in which a novel constellation of the two above parameters leads to an unusually high CO₂ permeability. Mitochondrial membranes (inner as well as outer) have an extremely low cholesterol content, amounting to an about 40-fold lower value compared to the cholesterol levels in plasma membranes [34, 35]. This per se is expected to impart a high P_{M,CO_2} to the mitochondrial membrane, which on the basis of the data of Itel et al. [3] can easily assume the value reported here, 0.3 cm/s. On the other hand, the mitochondrial membrane does not seem to possess any known protein gas channel. This is compatible with the lack of an effect of DIDS on P_{M,CO_2} as seen in Fig. 5; DIDS has been shown to be an effective gas channel inhibitor [16] both for aquaporin 1 and for Rhesus-associated glycoprotein [5, 6]. Furthermore, while many aquaporin isoforms have been shown to function as protein gas channels [36], the

only isoform known to be present in mitochondria, aquaporin 8 [37, 38], does not conduct CO₂ [36]. The available evidence thus points to the mitochondrial membrane exhibiting a very high CO₂ permeability due to extremely low cholesterol content in spite of the absence of gas channels.

Acknowledgments

We thank the Deutsche Forschungsgemeinschaft for support of this project under grant No. EN 908/2-1. MAH thanks the Deutscher Akademischer Austauschdienst and the University of Costa Rica for financial support.

Disclosure Statement

None of the authors declares any conflict of interest.

References

- 1 Elder JA, Lehninger AL: Respiration-dependent transport of carbon dioxide into rat liver mitochondria. *Biochemistry* 1973;12:976-982.
- 2 Balboni E, Lehninger AL: Entry and exit pathways of CO₂ in rat liver mitochondria respiring in a bicarbonate buffer system. *J Biol Chem* 1986;261:3563-3570.
- 3 Itel F, Al-Samir S, Öberg F, Chami M, Kumar M, Supuran CT, Deen PMT, Meier W, Hedfalk K, Gros G, Endeward V: CO₂ permeability of cell membranes is regulated by membrane cholesterol and protein gas channels. *FASEB J* 2012;26:5182-5191.
- 4 Endeward V, Gros G: Low carbon dioxide permeability of the apical epithelial membrane of guinea-pig colon. *J Physiol* 2005;15:253-265.
- 5 Endeward V, Musa-Aziz R, Cooper GJ, Chen LM, Pelletier MF, Virkki LV, Supuran CT, King LS, Boron WF, Gros G: Evidence that aquaporin 1 is a major pathway for CO₂ transport across the human erythrocyte membrane. *FASEB J* 2006;20:1974-1981.
- 6 Endeward V, Cartron JP, Ripoche P, Gros G: RhAG protein of the Rhesus complex is a CO₂ channel in the human red cell membrane. *FASEB J* 2008;22:64-73.
- 7 Endeward V, Al-Samir S, Itel F, Gros G: How does carbon dioxide permeate cell membranes? A discussion of concepts, results and methods. *Front Physiol* 2014;4:382.
- 8 Vincent SH, Silverman DN: Carbonic anhydrase activity in mitochondria from rat liver. *J Biol Chem* 1982; 257: 6850-6855.
- 9 Dodgson SJ, Forster RE, Storey BT, Mela L: Mitochondrial carbonic anhydrase. *Proc Natl Acad Sci USA* 1980;77:5562-5566.
- 10 Ono Y, Lin L, Storey BT, Taguchi Y, Dodgson SJ, Forster RE: Continuous measurement of ¹³C₁₆O₂ production from [¹³C] pyruvate by intact liver mitochondria: effect of HCO₃⁻. *Am J Physiol* 1996;270:C98-C106.
- 11 Fernández-Vizarrá E, Lopez-Perez MJ, Enriquez JA: Isolation of biogenetically competent mitochondria from mammalian tissues and cultured cells. *Methods* 2002;26:292-297.
- 12 Fernández-Vizarrá E, Ferrín G, Pérez-Martos A, Fernández-Silva P, Zeviani M, Enriquez JA: Isolation of mitochondria for biogenetical studies: An update. *Mitochondrion* 2010;10:253-262.
- 13 Schwerzmann K, Cruz-Orive LM, Eggman R, Sängler A, Weibel ER: Molecular architecture of the inner membrane of mitochondria from rat liver: a combined biochemical and stereological study. *J Cell Biol* 1986;102:97-103.
- 14 Reynolds ES: The use of lead citrate at high pH as an electron-opaque stain in electron microscopy. *J Cell Biol* 1963;17:208-213.

- 15 Perut F, Carta F, Bonuccelli G, Grisendi G, Di Pompo G, Avnet S, Sbrana FV, Hosogi S, Dominici M, Kusuzaki K, Supuran CT, Baldini N: Carbonic anhydrase IX inhibition is an effective strategy for osteosarcoma treatment. *Expert Opin Ther Targets* 2015;19:1593-1605.
- 16 Forster RE, Gros G, Lin L, Ono Y, Wunder M: The effect of 4,4'-diisothiocyanato-stilbene-2,2'-disulfonate on CO₂ permeability of the red blood cell membrane. *Proc Natl Acad Sci USA* 1998;95:15815-15820.
- 17 Traaseth N, Elfering S, Solien J, Haynes V, Giulivi C: Role of calcium signaling in the activation of mitochondrial nitric oxide synthase and citric acid cycle. *Biochim Biophys Acta* 2004;1658:64-71.
- 18 Kantrow SP, Taylor DE, Carraway MS, Piantadosi CA: Oxidative metabolism in rat hepatocytes and mitochondria during sepsis. *Arch Biochem Biophys* 1997;345:278-288.
- 19 Alberts B, Johnson A, Lewis J, Raff M, Roberts K, Walter P: *Molekularbiologie der Zelle*. John Wiley & Sons, 2011.
- 20 Halestrap A, Quinlan PT: The intramitochondrial volume measured using sucrose as an extramitochondrial marker overestimates the true matrix volume determined with mannitol. *Biochem J* 1983;214:387-393.
- 21 Cohen NS, Cheung C, Raijman L: Measurements of mitochondrial volumes are affected by the amount of mitochondria used in the determinations. *Biochem J* 1987;245:375-379.
- 22 Williams GR: Dynamic aspects of the tricarboxylic acid cycle in isolated mitochondria. *Can J Biochem* 1965;43:603-615.
- 23 Itada N, Forster RE: Carbonic anhydrase activity in intact red blood cells measured with 18O exchange. *J Biol Chem* 1977;252:3881-3890.
- 24 Dodgson SJ, Forster RE: Carbonic anhydrase activity of intact erythrocytes from seven mammals. *J Appl Physiol Respir Environ Exerc Physiol* 1983;55:1292-1298.
- 25 Al-Samir S, Papadopoulos S, Scheibe RJ, Meißner JD, Cartron JP, Sly WS, Alper SL, Gros G, Endeward V: Activity and distribution of intracellular carbonic anhydrase II and their effects on the transport activity of anion exchanger AE1/SLC4A1. *J Physiol* 2013;591:4963-4982.
- 26 Peters T, Forster RE, Gros G: Hagfish (*Myxine Glutinosa*) red cell membrane exhibits no bicarbonate permeability as detected by 18O exchange. *J Exp Biol* 2000; 203: 1551-1560.
- 27 Chappel JB, Crofts AR: In Regulation of Metabolic Processes in Mitochondria. Tager JM, Papa S, Quagliariello E and Slater EC (eds). Elsevier, Amsterdam, 1966, pp. 293-314.
- 28 Guarino RD, Dike LE, Haq TA, Rowley JA, Pitner JB, Timmins MR: Method for determining oxygen consumption rates of static cultures from microplate measurements of pericellular dissolved oxygen concentration. *Biotechnol Bioeng* 2004;86:775-787. Erratum in: *Biotechnol Bioeng* 2005;91:392.
- 29 Hub JS, Winkler FK, Merrick M, de Groot BL: Potentials of mean force and permeabilities for carbon dioxide, ammonia, and water flux across a Rhesus protein channel and lipid membranes. *J Am Chem Soc* 2010;132:13251-13263.
- 30 Kai L, Kaldenhoff R: A refined model of water and CO₂ membrane diffusion: effects and contribution of sterols and proteins. *Sci Rep* 2014;4:6665.
- 31 Tsiavaliaris G, Itef F, Hedfalk K, Al-Samir S, Meier W, Gros G, Endeward V: Low CO₂ permeability of cholesterol-containing liposomes detected by stopped-flow fluorescence spectroscopy. *FASEB J* 2015;29:1780-1793.
- 32 Khelashvili G, Johnner N, Zhao G, Harries D, Scott HL: Molecular origins of bending rigidity in lipids with isolated and conjugated double bonds: the effect of cholesterol. *Chem Phys Lipids* 2014;178:18-26.
- 33 Hill WG, Zeidel ML: Reconstituting the barrier properties of a water-tight epithelial membrane by design of leaflet-specific liposomes. *J Biol Chem* 2000;275:30176-30185.
- 34 Horvath SE, Daum G: Lipids of mitochondria. *Prog Lipid Res* 2013;52:590-614.
- 35 Paradies G, Ruggiero FM: Effect of aging on the activity of the phosphate carrier and on the lipid composition in rat liver mitochondria. *Arch Biochem Biophys* 1991;284:332-337.
- 36 Geyer R, Musa-Aziz R, Qin X, Boron WF: Relative CO₂/NH₃ selectivities of mammalian aquaporins 0-9. *Am J Physiol Cell Physiol* 2013;304:985-994.
- 37 Calamita G, Ferri D, Gena P, Liquori GP, Cavalier A, Thomas D, Svelto M: The inner mitochondrial membrane has aquaporin-8 water channels and is highly permeable to water. *J Biol Chem* 2005;280:17149-17153.
- 38 Molinas SM, Trumper L, Marinelli RA: Mitochondrial aquaporin-8 in renal proximal tubule cells: evidence for a role in the response to metabolic acidosis. *Am J Physiol Renal Physiol* 2012;303:F458-F466.